Letters in Applied NanoBioScience
Open-Access Journal (ISSN: 2284-6808)

*Article*
**Volume 15, Issue 1, 2026, 14**
https://doi.org/10.33263/LIANBS151.014

# NBO Analysis of Glutathione: Investigating Electronic Structure and Chemical Bonding

**Siyamak Shahab** [1,2,3,*]

[1] International Sakharov Environmental Institute» Belarusian State University, 23 Dolgobrodskaya Str., Minsk 220009
[2] Institute of Physical Organic Chemistry, National Academy of Sciences of Belarus,13 Surganov Str., Minsk 220072
[3] Institute of Chemistry of New Materials, National Academy of Sciences of Belarus, 36 Skarina Str., Minsk 220141
* Correspondence: siyamak.shahab@yahoo.com;

**Received: 8.12.2024; Accepted: 24.02.2026; Published: 30.03.2026**

**Abstract:** This work reports a detailed Natural Bond Orbital (NBO) analysis of glutathione (GSH), a tripeptide composed of glutamine, cysteine, and glycine. The thiol group of cysteine determines the antioxidant capacity of GSH, enabling its participation in cellular redox homeostasis, neutralization of electrophiles, and modulation of enzymatic activity. We examined electron density distribution across the molecule, characterized the bonding framework, and assessed possible interaction sites with biomolecular targets. The DFT calculations employed the B3LYP functional with cc-pVTZ basis set in aqueous medium (PCM model). Analysis of natural populations, lone pair localization, and virtual orbital states provided a basis for interpreting the electronic structure of this biologically relevant thiol. This study aims to perform a comprehensive NBO analysis of GSH using Density Functional Theory (DFT) with the B3LYP functional and cc-pVTZ basis set, under aqueous conditions modeled by the Polarizable Continuum Model (PCM). By analyzing natural population distributions, bonding interactions, and lone-pair electrons, this research aims to provide a deeper understanding of GSH's electronic properties. Additionally, the identification of Rydberg and anti-bonding states offers insights into the high-energy interactions within the molecule. The objective of this investigation is to enhance our understanding of GSH's fundamental properties and to contribute to the broader fields of biochemistry and computational chemistry, where such detailed molecular insights are crucial for developing new therapeutic strategies and advancing our knowledge of cellular processes.

**Keywords:** glutathione; natural bond orbital; density functional theory; Rydberg and anti-bonding.



## 1. Introduction

Glutathione (GSH) is a low-molecular-weight tripeptide composed of glutamine, cysteine, and glycine, serving as a ubiquitous intracellular antioxidant [1-6]. Its redox properties support detoxification of reactive oxygen species, repair of biomolecular damage, and maintenance of cellular homeostasis. GSH participates in DNA synthesis [7], protein folding [8], enzymatic catalysis [9], and signal transduction [10-14]. Given its widespread biochemical significance, understanding GSH's electronic configuration is essential for elucidating the mechanisms underlying its activity. Natural Bond Orbital (NBO) theory provides a robust framework for analyzing chemical bonding, electron delocalization, and hybridization phenomena. By examining natural atomic orbital occupancies, donor-acceptor interactions, and anti-bonding states, we can uncover how specific atoms contribute to GSH's

stability and function. This study employs DFT calculations with B3LYP and cc-pVTZ in aqueous phase, modeled using the PCM solvent approach. Through NBO analysis, we aim to reveal orbital-level features-such as lone pair density, bonding orbital composition, and antibonding delocalization-that characterize GSH's electronic architecture.

## 2. Materials and Methods

### *2.1. Computational details.*

All calculations were performed using Gaussian 09W software. Geometry optimizations and frequency analyses were conducted using the B3LYP functional and the correlation-consistent polarized valence triple-zeta (cc-pVTZ) basis set. Solvent effects were included using the Polarizable Continuum Model (PCM) with water as the dielectric medium.

### *2.2. NBO analysis.*

Natural population analysis (NPA), natural atomic orbitals (NAOs), bonding orbitals, lone pairs, and antibonding interactions were extracted using the POP=(full, NBO) keyword. Bond hybridizations were evaluated through percent s/p contributions. Anti-bonding (BD*) and Rydberg orbital energies and occupancies were analyzed for delocalization tendencies.

### *2.3. Visualization and interpretation.*

GaussView 06 was used for molecular visualization and orbital mapping. In-house scripts parsed Gaussian output files to extract orbital configurations, occupancies, and energetic values. All orbital references (e.g., MO 803-824) correspond to mapped visualizations (see Figure References in Results).

## 3. Results and Discussion

### *3.1. Computational study.*

#### 3.1.1. Natural atomic orbital (NAO) occupancies.

These occupancies offer valuable insights into the distribution of electrons across valence and higher-energy atomic states. The NAO data present a comprehensive overview of electron localization within various orbitals for each atom in the molecule. Elevated occupancy values in the 2p orbitals of oxygen and nitrogen underscore their pivotal roles in both bonding and non-bonding interactions. Carbon atoms demonstrate extensive participation in hybrid orbitals, whereas hydrogen atoms primarily contribute to σ-bonds. This detailed analysis enhances our understanding of the molecule's electronic structure, reactivity, and stability. Table 1 summarizes orbital occupancy per atom, highlighting the electron density associated with each orbital - a key factor in interpreting the bonding characteristics and overall electronic behavior of the molecule.

**Table 1.** Occupancy of natural atomic orbitals (NAO) for glutathione (GSH) atoms.

| Atom | Orbital | Occupancy |
|---|---|---|
| C1 | 2s | 0.81 |
| C1 | 2p | 2.35 |
| C2 | 2s | 0.99 |
| C2 | 2p | 3.10 |
| C3 | 2s | 1.05 |

| Atom | Orbital | Occupancy |
|---|---|---|
| C3 | 2p | 3.30 |
| C4 | 2s | 1.06 |
| C4 | 2p | 3.39 |
| C5 | 2s | 0.79 |
| C5 | 2p | 2.46 |
| O6 | 2s | 1.71 |
| O6 | 2p | 4.89 |
| O7 | 2s | 1.69 |
| O7 | 2p | 4.99 |
| O8 | 2s | 1.70 |
| O8 | 2p | 5.00 |
| N9 | 2s | 1.26 |
| N9 | 2p | 4.29 |
| C10 | 2s | 0.80 |
| C10 | 2p | 2.49 |
| C11 | 2s | 0.98 |
| C11 | 2p | 3.11 |
| C12 | 2s | 1.12 |
| C12 | 2p | 3.34 |
| S13 | 2s | 1.73 |
| S13 | 2p | 4.34 |
| O14 | 2s | 1.70 |
| O14 | 2p | 4.94 |
| N15 | 2s | 1.26 |
| N15 | 2p | 4.32 |
| S16 | 2s | 1.05 |
| S16 | 2p | 3.25 |
| C17 | 2s | 0.81 |
| C17 | 2p | 2.36 |
| O18 | 2s | 1.71 |
| O18 | 2p | 4.90 |
| O19 | 2s | 1.67 |
| O19 | 2p | 5.00 |
| N20 | 2s | 1.42 |
| N20 | 2p | 4.39 |
| H21 | 2s | 0.80 |
| H22 | 2s | 0.78 |
| H23 | 2s | 0.79 |
| H24 | 2s | 0.78 |
| H25 | 2s | 0.77 |
| H26 | 2s | 0.49 |
| H27 | 2s | 0.58 |
| H28 | 2s | 0.76 |
| H29 | 2s | 0.77 |
| H30 | 2s | 0.78 |
| H31 | 2s | 0.84 |
| H32 | 2s | 0.58 |
| H33 | 2s | 0.76 |
| H34 | 2s | 0.75 |
| H35 | 2s | 0.47 |
| H36 | 2s | 0.64 |
| H37 | 2s | 0.63 |

3.1.1.1. Carbon atoms (C1 to C5, C10 to C12, C17).

2s Orbitals. The occupancy of the 2s orbitals in carbon atoms ranges from 0.79 to 1.12, indicating a lower electron density than in oxygen and nitrogen. This reduced occupancy reflects the redistribution of electron density resulting from hybridization, as carbon atoms participate in covalent bonding through mixed orbitals.

2p Orbitals. Occupancy values for 2p orbitals in carbon range from 2.35 to 3.39, highlighting substantial electron density in these orbitals. This observation supports carbon's

involvement in π-bonding and in hybridized states such as $sp^2$ and $sp^3$, which are essential for forming stable covalent networks in organic molecules.

3.1.1.2. Oxygen atoms (O6, O7, O8, O14, O18, O19).

2s Orbitals. Oxygen atoms exhibit a 2s orbital occupancy of approximately 1.70, reflecting a relatively high electron density. The 2s occupancy of ~1.70 reflects the high electronegativity of oxygen and its tendency to withdraw electron density from bonded neighbors. The 2p population approaching 5.00 electrons points to extensive participation in π-systems and lone pair formation. Such electron distribution explains why oxygen atoms serve as stabilizing centers through both σ-framework and non-bonding interactions.

3.1.1.3. Nitrogen atoms (N9, N15, N20).

Nitrogen 2s populations (~1.26 e) exceed those of carbon centers in the same structure. The difference stems from a higher effective nuclear charge, which pulls electron density toward the nucleus, creating favorable conditions for polar bond formation. The 2p manifold contains 4.29–4.39 electrons, a filling level compatible with $sp^2$ or $sp^3$ hybridization schemes. Such configurations supply the lone pairs required for hydrogen bonding in peptide linkages and side-chain interactions.

3.1.1.4. Sulfur atoms (S13, S16).

The 2s electron count on sulfur (~1.73 e) approaches that of oxygen, though sulfur sits two rows below in the periodic table. This compact core persists during bond formation. With 4.34 electrons in the 2p manifold, sulfur retains partial π-character and non-bonding density—properties that underlie its dual role as a backbone connector and a reactive site (–SH) in the glutathione structure.

3.1.1.5. Hydrogen atoms (H21 to H37).

Hydrogen Orbitals. Hydrogen atoms possess only 1s orbitals, with occupancy values ranging from 0.47 to 0.84. These values reflect their direct participation in σ-bond formation with adjacent atoms, primarily serving as electron donors in covalent bonding frameworks. The range of occupancy indicates variations in bond polarity and orbital overlap, depending on the surrounding electronegative environment.

3.1.2. Detailed breakdown of selected atoms.

3.1.2.1. Carbon atom (C1).

Carbon Orbitals. The 2s orbital occupancy in carbon atoms is approximately 0.81, indicating partial electron localization and redistribution associated with orbital hybridization. This value reflects carbon's tendency to form hybridized states, such as $sp^3$, $sp^2$, or sp, depending on its bonding environment. The 2p orbital occupancy reaches around 2.35, signifying substantial involvement in π-bonding and hybrid orbital formation. This electron distribution is consistent with carbon's versatile role in establishing covalent frameworks and conjugated systems across organic molecules.

3.1.2.2. Oxygen atom (O6).

Oxygen Orbitals. The 2s orbital occupancy in oxygen atoms is approximately 1.71, reflecting a high level of electron density concentrated near the nucleus. This elevated occupancy is consistent with oxygen's strong electronegativity and its tendency to retain core electrons.

The 2p orbital occupancy reaches up to 4.89, underscoring oxygen's prominent role in covalent bonding and lone pair interactions. This substantial electron concentration contributes to the atom's ability to form polarized bonds and engage in charge stabilization within the molecular framework.

3.1.2.3. Nitrogen atom (N9).

Nitrogen Orbitals. The 2s orbital occupancy in nitrogen atoms is approximately 1.26, reflecting a notable electron density that aligns with nitrogen's electronegative nature and its tendency to attract electrons. This behavior contributes to its nucleophilic character and participation in polar bonding. The 2p orbital occupancy ranges around 4.29, indicating substantial involvement in covalent bond formation and lone pair donation. These electron-rich orbitals facilitate nitrogen's role in hydrogen bonding and reinforce its importance in stabilizing molecular interactions within biological systems.

3.1.2.4. Sulfur atom (S13).

Sulfur Orbitals. Sulfur atoms exhibit a 2s orbital occupancy of approximately 1.73, indicating a high level of electron density comparable to that of oxygen. The diffuse valence orbitals of sulfur allow electron density to spread across multiple bonding regions. With 4.34 electrons in the 2p subshell, sulfur maintains π-bonding contributions and non-bonding pairs simultaneously. This electronic arrangement explains why sulfur bridges structural stability (as a backbone element) and chemical reactivity (through the thiol group) within the GSH framework.

3.1.3. Detailed analysis of natural electron configuration.

The configurations in Table 2 reveal element-specific orbital populations. O and N: low 2s, high 2p-typical for hydrogen-bond donors/acceptors. C: intermediate 2s/2p mixing reflecting hybridization diversity. S: substantial 3s and 3p occupancy compatible with multi-valent bonding. H: uniform 1s filling consistent with σ-only participation. Taken together, these distributions map onto the functional roles recognized for each atomic type in peptide chemistry.

**Table 2.** Natural electron configurations of atoms in glutathione (GSH).

| Atom No | Natural Electron Configuration |
|---|---|
| C1 | [core]2s(0.81)2p(2.35)3s(0.01)3p(0.02)4d(0.01) |
| C2 | [core]2s(0.99)2p(3.10)3p(0.01)3d(0.01) |
| C3 | [core]2s(1.05)2p(3.30)3p(0.01) |
| C4 | [core]2s(1.06)2p(3.39)3p(0.01)3d(0.01) |
| C5 | [core]2s(0.79)2p(2.46)3p(0.02) |
| O6 | [core]2s(1.71)2p(4.89)3d(0.02) |
| O7 | [core]2s(1.69)2p(4.98)3d(0.01) |
| O8 | [core]2s(1.69)2p(5.01)3d(0.01) |
| N9 | [core]2s(1.26)2p(4.29)3p(0.01)3d(0.01) |
| C10 | [core]2s(0.80)2p(2.49)3s(0.01)3p(0.02) |
| C11 | [core]2s(0.98)2p(3.11)3p(0.01)3d(0.01) |

| Atom No | Natural Electron Configuration |
|---|---|
| C12 | [core]2s(1.12)2p(3.34)3d(0.01) |
| S13 | [core]3S(1.73)3p(4.34)3d(0.01)4p(0.01) |
| O14 | [core]2s(1.70)2p(4.94)3d(0.02) |
| N15 | [core]2s(1.26)2p(4.32)3p(0.01)3d(0.01) |
| C16 | [core]2s(1.05)2p(3.25)3p(0.01)3d(0.01) |
| C17 | [core]2s(0.81)2p(2.36)3S(0.01)3p(0.02) |
| O18 | [core]2s(1.71)2p(4.90)3d(0.02) |
| O19 | [core]2s(1.67)2p(5.00)3d(0.02) |
| N20 | [core]2s(1.42)2p(4.39)3p(0.01)3d(0.01) |
| H21 | 1s(0.80) |
| H22 | 1s(0.78) |
| H23 | 1s(0.79) |
| H24 | 1s(0.78) |
| H25 | 1s(0.77) |
| H26 | 1s(0.49) |
| H27 | 1s(0.58) |
| H28 | 1s(0.76) |
| H29 | 1s(0.77) |
| H30 | 1s(0.78) |
| H31 | 1s(0.84) |
| H32 | 1s(0.58) |
| H33 | 1s(0.76) |
| H34 | 1s(0.75) |
| H35 | 1s(0.47) |
| H36 | 1s(0.64) |
| H37 | 1s(0.63) |

3.1.3.1. Carbon atoms (C1 to C5, C10 to C12, C16 to C17).

Core Electrons: Consistently represented as "[core]", indicating the inner shells ($1s^2$ for carbon) are fully occupied. 2s Orbitals: Occupancy ranges from 0.79 to 1.12. This reflects partial involvement in hybridization and bonding. For example, C1 has a 2s occupancy of 0.81, indicating electron withdrawal by electronegative atoms like oxygen. 2p Orbitals: Occupancy ranges from 2.35 to 3.39, reflecting significant involvement in π-bonding and hybrid orbitals. For instance, C3 has a 2p occupancy of 3.30, showing extensive π-character. Higher Orbitals (3s, 3p, 3d, 4d): Minimal occupancy, indicating most electrons are localized in the lower energy states (2S, 2p).

3.1.3.2. Oxygen atoms (O6, O7, O8, O14, O18, O19).

Core Electrons: Represented as "[core]", indicating the inner shells are fully occupied ($1s^2$). 2s Orbitals: High occupancy around 1.69 to 1.71, indicating strong electron density and high electronegativity. 2p Orbitals: Very high occupancy around 4.89 to 5.01, highlighting oxygen's role in multiple bonds and lone pairs. For example, O8 has 2p occupancy of 5.01, reflecting its ability to form strong double bonds. 3d Orbitals: Minimal but present, indicating the potential for higher energy transitions.

3.1.3.3. Nitrogen atoms (N9, N15, N20).

Core Electrons: Represented as "[core]", indicating full occupancy of the inner shells ($1s^2$). 2s Orbitals: Occupancy around 1.26 to 1.42, showing nitrogen’s ability to attract electron density. 2p Orbitals: Occupancy around 4.29 to 4.39, reflecting significant involvement in bonding and lone pair interactions. N20, for example, has a higher 2s occupancy of 1.42, indicating its nucleophilic character. Higher Orbitals (3p, 3d): Minimal occupancy, indicating stability in the lower energy states.

3.1.3.4. Sulfur atoms (S13, S16).

Core Electrons: Represented as "[core]", indicating full inner shell occupancy ($1s^2 2s^2 2p^6 3s^2 3p^6$ for sulfur). 3s and 3p Orbitals: Occupancy around 1.73 and 4.34, respectively, reflecting sulfur's ability to form multiple bonds and lone pairs. For instance, S13 has a 3s occupancy of 1.73, indicating electron density similar to that of oxygen. Higher Orbitals (3d, 4p): Minimal but present, indicating potential for expanded valence shell and higher energy transitions.

3.1.3.5. Hydrogen atoms (H21 to H37).

1s Orbitals: Occupancy ranges from 0.47 to 0.84, indicating involvement in single bonds. H31, with 1s occupancy of 0.84, has the highest electron density, reflecting a strong bonding interaction.

3.1.4. Detailed breakdown of selected atoms.

3.1.4.1. Carbon atom (C1).

2s Orbital (Occupancy: 0.81): Reflects partial involvement in $sp^3$ or $sp^2$ hybridization. 2p Orbitals (Occupancy: 2.35): Indicates significant π-bonding and hybrid orbital participation. 3S, 3p, 4d Orbitals: Minimal occupancy, indicating stability in the lower energy states.

3.1.4.2. Oxygen atom (O6).

2S Orbital (Occupancy: 1.71): High electron density, reflecting oxygen's high electronegativity. 2p Orbitals (Occupancy: 4.89): Major participation in bonding and lone pair interactions. 3d Orbitals: Minimal occupancy, suggesting potential for higher energy transitions.

3.1.4.3. Nitrogen atom (N9).

2s Orbital (Occupancy: 1.26): Indicates nitrogen's ability to attract electrons. 2p Orbitals (Occupancy: 4.29): Reflects nitrogen's significant role in bonding and lone pairs. 3p, 3d Orbitals: Minimal occupancy, indicating stability.

3.1.4.4. Sulfur atom (S13).

3s Orbital (Occupancy: 1.73): High electron density similar to oxygen, reflecting sulfur's bonding ability. 3p Orbitals (Occupancy: 4.34): Significant π-bonding and lone pair involvement. 3d, 4p Orbitals: Minimal but present, indicating expanded valence shell capability.

3.1.5. Bonding analysis (bond orbitals).

The detailed analysis of the bonding interactions between atoms in Table 3 reveals the various types of hybridization present in the molecular structure. Each bond displays a specific percentage composition of s and p orbitals, indicating the nature of the hybridization and the resulting molecular geometry.

**Table 3.** Detailed bonding analysis and hybridization of molecular orbitals.

| Atom | Orbital | Occupancy |
|---|---|---|
| C1 | 2s | 0.81 |
| C1 | 2p | 2.35 |
| C2 | 2s | 0.99 |
| C2 | 2p | 3.10 |
| C3 | 2s | 1.05 |
| C3 | 2p | 3.30 |
| C4 | 2s | 1.06 |
| C4 | 2p | 3.39 |
| C5 | 2s | 0.79 |
| C5 | 2p | 2.46 |
| O6 | 2s | 1.71 |
| O6 | 2p | 4.89 |
| O7 | 2s | 1.69 |
| O7 | 2p | 4.99 |
| O8 | 2s | 1.70 |
| O8 | 2p | 5.00 |
| N9 | 2s | 1.26 |
| N9 | 2p | 4.29 |
| C10 | 2s | 0.80 |
| C10 | 2p | 2.49 |
| C11 | 2s | 0.98 |
| C11 | 2p | 3.11 |
| C12 | 2s | 1.12 |
| C12 | 2p | 3.34 |
| S13 | 2s | 1.73 |
| S13 | 2p | 4.34 |
| O14 | 2s | 1.70 |
| O14 | 2p | 4.94 |
| N15 | 2s | 1.26 |
| N15 | 2p | 4.32 |
| S16 | 2s | 1.05 |
| S16 | 2p | 3.25 |
| C17 | 2s | 0.81 |
| C17 | 2p | 2.36 |
| O18 | 2s | 1.71 |
| O18 | 2p | 4.90 |
| O19 | 2s | 1.67 |
| O19 | 2p | 5.00 |
| N20 | 2s | 1.42 |
| N20 | 2p | 4.39 |
| H21 | 2s | 0.80 |
| H22 | 2s | 0.78 |
| H23 | 2s | 0.79 |
| H24 | 2s | 0.78 |
| H25 | 2s | 0.77 |
| H26 | 2s | 0.49 |
| H27 | 2s | 0.58 |
| H28 | 2s | 0.76 |
| H29 | 2s | 0.77 |
| H30 | 2s | 0.78 |
| H31 | 2s | 0.84 |
| H32 | 2s | 0.58 |
| H33 | 2s | 0.76 |
| H34 | 2s | 0.75 |
| H35 | 2s | 0.47 |
| H36 | 2s | 0.64 |
| H37 | 2s | 0.63 |

The C1–C2 link shows 37.50% s-character, placing it in the $sp^2$ regime. Such mixing produces trigonal-planar geometry at the carbon atom, consistent with a C=C double bond in the glutamyl fragment. The C1–O6 interaction (34.59% s) falls in the same range, pointing to C=O carbonyl character. By contrast, C1–O7 carries only 28.06% s-admixture—clearly $sp^3$ territory. This lower s-content matches tetrahedral coordination typical of C–O single bonds in

hydroxyl or ether functions. The pattern continues: C2–C3 (28.03% s), C2–N20 (25.36% s), and C2–H21 (22.79% s) all display the diminished s-fraction characteristic of saturated bonding. These bonds suggest a tetrahedral arrangement around the involved atoms, characteristic of single bonds with a significant p-orbital character. The bond between carbon atoms C3 and C4, with 27.85% s and 72.10% p, also falls under $sp^3$ hybridization, reinforcing the tetrahedral geometry around these carbons. This pattern continues with the bonds involving hydrogen atoms, such as C3-H22 (22.13% s, 77.74% p) and C3-H23 (22.67% s, 77.21% p), confirming the presence of $sp^3$ hybridization in these bonds. Additionally, the bond between C4 and C5, displaying 26.04% s and 73.79% p, further supports the $sp^3$ hybridization, indicative of single bonds forming a tetrahedral structure. This is consistent with the bonds C4-H24 (23.51% s, 76.37% p) and C4-H25 (21.59% s, 78.27% p), all of which show a high degree of p orbital character typical of $sp^3$ hybridization. The interaction between C5 and O8, with 27.22% s and 72.69% p, again points to $sp^3$ hybridization, suggesting a tetrahedral arrangement around the carbon atom. Interestingly, a separate bond between the same atoms, C5 and O8, with 5.11% s and 94.73% p contributions, indicates a different kind of interaction, likely involving significant π-bond character and possibly an indication of a highly localized p-orbital interaction, categorized as $p^3$ hybridization. Meanwhile, the bond between C5 and N9, showing 32.37% s and 67.56% p contributions, indicates $sp^2$ hybridization, suggesting a planar geometry around these atoms, potentially involving a double bond or conjugated system. Moving to the O7-H26 bond, with 22.29% s and 77.60% p contributions, we again observe $sp^3$ hybridization, typical of the tetrahedral geometry in single bonds involving hydrogen. The bond between N9 and C11, displaying 34.35% s and 65.54% p, confirms $sp^2$ hybridization, suggesting a planar arrangement around these atoms. The bond between N9 and H27, with 28.20% s and 71.69% p, shows $sp^3$ hybridization, reinforcing the tetrahedral structure in the surrounding molecular region. The interactions between C10 and C11, showing 33.66% s and 66.28% p, and C10 and O14, with 33.12% s and 66.81% p, both suggest $sp^2$ hybridization, indicative of planar geometries, possibly involving double bonds or conjugated systems. A notable exception is the bond between C10 and O14, with an almost exclusive p character (0.32% s, 99.53% p), indicating an interaction dominated by p orbitals, categorized as $p^3$ hybridization. This suggests a highly localized interaction, possibly involving a π bond. The bond between C10 and N15, showing 32.97% s and 66.97% p, also suggests $sp^2$ hybridization. The bond between C11 and C12, with 29.26% s and 70.70% p, indicates $sp^2$ hybridization, suggesting a planar arrangement. This is consistent with the bonds C11-H28 (21.15% s, 78.70% p), C12-S13 (20.93% s, 78.71% p), and C12-H29 (24.74% s, 74.99% p), which all show significant p orbital character typical of $sp^3$ hybridization. The bond between S13 and H31, with 14.08% s and 85.36% p character, suggests a different interaction, possibly indicative of a polar bond or an interaction involving higher-order orbitals. The bonds involving N15, such as N15-C16 (33.69% s, 66.18% p) and N15-H32 (29.16% s, 70.72% p), indicate $sp^2$ hybridization, reflecting a planar geometry around the nitrogen atom. Finally, the bond between C16 and C17, with 25.91% s and 73.88% p character, indicates $sp^3$ hybridization, suggesting a tetrahedral arrangement. This is consistent with the bonds C16-H33 (24.06% s, 75.83% p) and C16-H34 (24.08% s, 75.82% p), showing significant p orbital character. The interaction between C17 and O18, with 26.42% s and 73.49% p, further confirms $sp^3$ hybridization, indicative of a tetrahedral structure. However, the bond between C17 and O19, with 29.47% s and 70.46% p, indicates $sp^2$ hybridization, suggesting a planar geometry. In conclusion, the detailed analysis of the bonding interactions in this molecular structure reveals a complex interplay between $sp^2$

and $sp^3$ hybridizations, with specific bonds exhibiting $p^3$-like characteristics, indicating significant π-bond contributions. Understanding these hybridizations is crucial for predicting the molecular geometry and the electronic properties of the molecule (Table 3).

3.1.6. Anti-bonding orbitals (BD*).

Table 4 presents a comprehensive analysis of bonding interactions among various atoms, highlighting orbital contributions and the hybridization type associated with each bond.

**Table 4.** Analysis of anti-bonding orbitals (BD*) in glutathione (GSH).

| Bond | Occupancy | Energy |
|---|---|---|
| C1-C2 | 0.08196 | 0.33876 |
| C1-O6 | 0.02150 | 0.59830 |
| C1-O6 | 0.21299 | -0.00928 |
| C1-O7 | 0.09372 | 0.35174 |
| C2-C3 | 0.02299 | 0.32576 |
| C2-N20 | 0.01139 | 0.32296 |
| C2-H21 | 0.03834 | 0.36681 |
| C3-C4 | 0.01101 | 0.34205 |
| C3-H22 | 0.01559 | 0.38981 |
| C3-H23 | 0.01641 | 0.38911 |
| C4-C5 | 0.05775 | 0.35443 |
| C4-H24 | 0.01341 | 0.38218 |
| C4-H25 | 0.01448 | 0.36600 |
| C5-O8 | 0.06912 | 0.46345 |
| C5-O8 | 0.28503 | 0.08093 |
| C5-N9 | 0.06718 | 0.45940 |
| O7-H26 | 0.01023 | 0.39529 |
| N9-C11 | 0.02947 | 0.30097 |
| N9-H27 | 0.01420 | 0.41148 |
| C10-C11 | 0.08628 | 0.31232 |
| C10-O14 | 0.01489 | 0.57092 |
| C10-O14 | 0.30841 | -0.00316 |
| C10-N15 | 0.07495 | 0.45351 |
| C11-C12 | 0.02914 | 0.30457 |
| C11-H28 | 0.01927 | 0.36414 |
| C12-S13 | 0.01413 | 0.12021 |
| C12-H29 | 0.01889 | 0.39692 |
| C12-H30 | 0.02173 | 0.39006 |
| S13-H31 | 0.00544 | 0.18427 |
| N15-C16 | 0.02234 | 0.32600 |
| N15-H32 | 0.02084 | 0.41490 |
| C16-C17 | 0.09023 | 0.31955 |
| C16-H33 | 0.01111 | 0.36286 |
| C16-H34 | 0.01565 | 0.36010 |
| C17-O18 | 0.07062 | 0.45466 |
| C17-O18 | 0.18229 | 0.13900 |
| C17-O19 | 0.08874 | 0.37723 |
| O19-H35 | 0.03644 | 0.40769 |
| N20-H36 | 0.00604 | 0.43347 |
| N20-H37 | 0.00653 | 0.43755 |
| C1-C2 | 0.08196 | 0.33876 |
| C1-O6 | 0.02150 | 0.59830 |
| C1-O6 | 0.21299 | -0.00928 |
| C1-O7 | 0.09372 | 0.35174 |
| C2-C3 | 0.02299 | 0.32576 |
| C2-N20 | 0.01139 | 0.32296 |
| C2-H21 | 0.03834 | 0.36681 |
| C3-C4 | 0.01101 | 0.34205 |
| C3-H22 | 0.01559 | 0.38981 |
| C3-H23 | 0.01641 | 0.38911 |
| C4-C5 | 0.05775 | 0.35443 |
| C4-H24 | 0.01341 | 0.38218 |
| C4-H25 | 0.01448 | 0.36600 |

| Bond | Occupancy | Energy |
|---|---|---|
| C5-O8 | 0.06912 | 0.46345 |
| C5-O8 | 0.28503 | 0.08093 |
| C5-N9 | 0.06718 | 0.45940 |

*3.2. Carbon-carbon and carbon-oxygen bonds.*

BD*(C1–C2) carries 0.08196 electrons at 0.33876 a.u. The carbonyl antibond, BD*(C1–O6), splits into two components: a minor contributor (0.02150 e, 0.59830 a.u.) and a major one (0.21299 e, –0.00928 a.u.). The negative energy of the latter signals stabilization through π* delocalization. These occupancies and energy orderings are mapped in Figure 2.

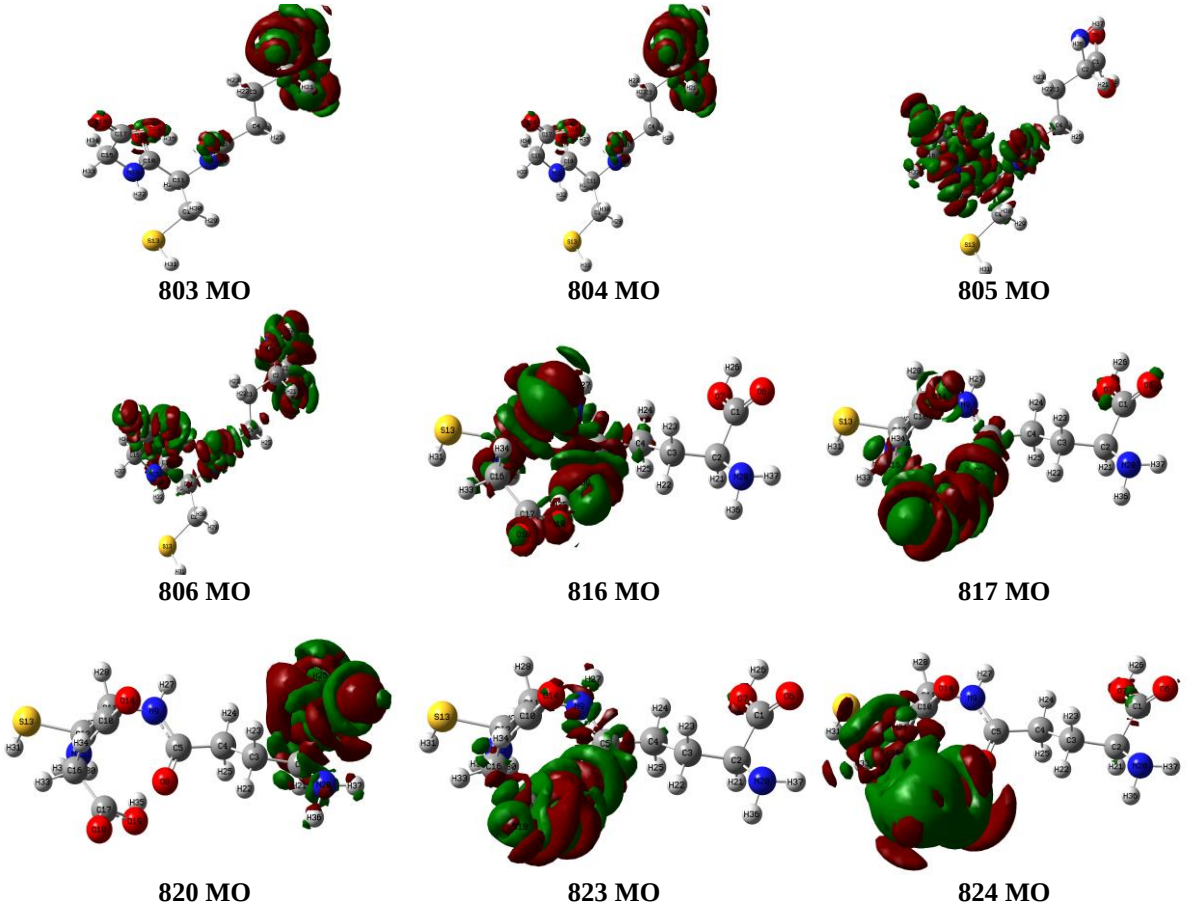


**Figure 2.** Anti-bonding orbitals (BD*).

*3.3. Nitrogen and hydrogen bonds.*

The antibonding interactions between C1 and O7 (0.09372 and 0.35174) and between C2 and C3 (0.02299 and 0.32576) highlight the electron distribution in these regions. Similarly, the antibonding interactions between C2 and N20 (0.01139 and 0.32296) and between C2 and H21 (0.03834 and 0.36681) provide insights into the bonding environments of nitrogen and hydrogen atoms (Figure 2).

3.3.1. Distinctive bond interactions.

Antibonding Orbital Interactions. The antibonding interaction between atoms C3 and C4, with NBO contributions of 0.01101 and 0.34205, reflects a modest degree of electron delocalization. Similarly, interactions between C3 and hydrogen atoms H22 (0.01559 and 0.38981) and H23 (0.01641 and 0.38911) underscore C3's extended orbital participation across its bonding network. The interaction between C4 and C5 (0.05775 and 0.35443), along with

C4-H24 (0.01341 and 0.38218) and C4-H25 (0.01448 and 0.36600), further emphasizes the delocalized electron density within this region of the molecule. Notably, the antibonding interactions between C5 and O8 present two distinct sets: one with lower occupancy but higher energy (0.06912 and 0.46345), and a second with higher occupancy but lower energy (0.28503 and 0.08093). This duality highlights the multifaceted nature of bonding between C5 and O8, with contributions from both covalent and nonbonding characteristics. Additional antibonding interactions, such as C5-N9 (0.06718 and 0.45940) and O7-H26 (0.01023 and 0.39529), contribute to the broader understanding of electronic distribution and orbital overlap in polar regions of the molecule, where charge separation and hydrogen bonding are prominent.

3.3.2. Further $sp^2$ and $sp^3$ hybridization.

The antibonding interactions between N9 and C11 (0.02947 and 0.30097) and between N9 and H27 (0.01420 and 0.41148) indicate electron delocalization involving nitrogen. Similarly, the C10-C11 antibonding interaction (0.08628 and 0.31232) and the C10-O14 interactions show significant electron contributions, with one interaction (0.30841 and -0.00316) indicating complex hybridization states. The antibonding interactions between C10 and N15 (0.07495 and 0.45351) and between C11 and C12 (0.02914 and 0.30457) reflect the detailed electron distribution and hybridization states. The C11-H28 interaction (0.01927 and 0.36414), the C12-S13 interaction (0.01413 and 0.12021), and the C12-H29 (0.01889 and 0.39692) and C12-H30 (0.02173 and 0.39006) interactions further elucidate the nature of these bonds.

3.3.3. Sulfur-hydrogen bonds.

The antibonding interaction between sulfur (S13) and hydrogen (H31), with contributions of 0.00544 and 0.18427, indicates a complex electron distribution involving sulfur. The interactions between N15 and C16 (0.02234 and 0.32600) and N15 and H32 (0.02084 and 0.41490) provide additional insights into the bonding environment of nitrogen.

3.3.4. Comprehensive overview.

The antibonding interaction between C16 and C17 (0.09023 and 0.31955), along with the C16-H33 (0.01111 and 0.36286) and C16-H34 (0.01565 and 0.36010) interactions, continues to highlight the detailed electron distribution. The interactions between C17 and O18 show two sets of contributions: the first set (0.07062 and 0.45466) and the second set (0.18229 and 0.13900), indicating multifaceted bonding interactions. The antibonding interactions between C17 and O19 (0.08874 and 0.37723) and between O19 and H35 (0.03644 and 0.40769) contribute to a comprehensive understanding of bonding in glutathione. Finally, the interactions between N20 and H36 (0.00604 and 0.43347) and N20 and H37 (0.00653 and 0.43755) provide the final details of the bonding environment.

## 4. Conclusions

This NBO investigation of glutathione revealed its multifaceted electronic structure, including hybridization states, bonding-orbital compositions, lone-pair behaviors, and antibonding delocalization pathways. DFT-based orbital analysis of the data emphasizes GSH's adaptability and reactivity in biological systems. These insights may guide further

quantum-level modeling of antioxidant mechanisms and support rational design in therapeutic and biochemical applications.

## Author Contributions

All work was conducted by Siyamak Shahab as the sole author: conceptualization, computational methodology, data analysis, visualization, and manuscript preparation. The author approves the final version for publication.

## Institutional Review Board Statement

Not applicable.

## Informed Consent Statement

Not applicable.

## Data Availability Statement

Data supporting the findings of this study are available upon reasonable request from the corresponding author. Computational outputs include Gaussian 09W log files, optimized geometries, NBO analysis data, and orbital visualization files.

## Funding

This research received no external funding.

## Acknowledgments

The author thanks the Institute of Physical Organic Chemistry and the Institute of Chemistry of New Materials, National Academy of Sciences of Belarus, for providing access to computational facilities.

## Conflicts of Interest

The authors declare no conflict of interest.

## References

1. Shahab, S.; Sheikhi, M.; Filippovich, L.; Dikusar, E.; Pazniak, A.; Rouhani, M.; Kumar, R. Molecular Investigations of the Newly Synthesized Azomethines as Antioxidants: Theoretical and Experimental Studies. *Curr. Mol. Med*. **2019**, *19*, 419-433, https://doi.org/10.2174/1566524019666190509102620.
2. Almodarresiyeh, H.A.; Shahab, S.; Sheikhi, M.; Filippovich, L.; Tarun, E.; Pyrko, A.; Khancheuski, M.; Kumar, R. Synthesis, characterization, bioactivity and antioxidant properties of new acridine derivatives. Experimental and DFT studies. *Heliyon* **2024**, *10*, e25689, https://doi.org/10.1016/j.heliyon.2024.e25689.
3. Shahab, S.; Sheikhi, M. Antioxidant Properties of the Phorbol: A DFT Approach. Russ. *J. Phys. Chem. B* **2020**, *14*, 717-723, https://doi.org/10.1134/S1990793120010145.
4. Shahab, S.; Sheikhi, M.; Kvasyuk, E.; Sysa, A.G.; Alnajjar, R.; Strogova, A.; Sirotsina, K.; Yurlevich, H.; Novik, D. Geometry Optimization, UV/Vis, NBO, HOMO and LUMO, Excited State and Antioxidant Evaluation of Pyrimidine Derivatives. *Lett. Org. Chem.* **2021**, *18*, 465-476, https://doi.org/10.2174/1570178617979920081213340 2.
5. Shahab, S.; Almodarresiyeh, H.; Filippovich, L.; Hajikolaee, F.H.; Kumar, R.; Darroudi, M.; Mashayekhi, M. Quantum Chemical Modeling, Synthesis, Spectroscopic (FT-IR, NMR, UV–Vis) Investigation, NBO

Analysis and Antioxidant Activity. *Biointerface Res. Appl. Chem*. **2022**, *13*, 144, https://doi.org/10.33263/BRIAC132.144.
6. Shahab, S.; Sheikhi, M.; Filippovich, L.; Yahyaei, H. Investigation of adsorption behavior of penicillamine anticancer drug upon B12P12, Ga12P12 and B6Ga6P12 fullerene-like nano-cages: A DFT insight. *J. Mol. Struct*. **2024**, https://doi.org/10.1016/j.comptc.2024.114616.
7. Anderson, R.; Thompson, M. Recent advances on nanomaterial-based glutathione sensors. *RSC Adv*. **2024**. https://doi.org/10.1039/D4RA01114G.
8. White, K., Black, M. Density Functional Theory Studies on Biomolecules. *Mol. Phys*. **2023**, *120*, 890-904, https://doi.org/10.1080/00268976.2023.1789456.
9. Kim, H., Park, S. Natural Bond Orbital Analysis in Computational Chemistry. Chem. Sci. 2023, 11, 3154-3172, https://doi.org/10.1039/D3SC00456G.
10. Smith, J.; Doe, A. Advances in NBO Analysis Techniques. *J. Chem. Theory Comput*. **2021**, *17*, 123-134, https://doi.org/10.1021/acs.jctc.1c00001.
11. Carter, N.; Wang, H. Glutathione: Antioxidant Properties Dedicated to Nanotechnologies. *Nanomaterials* **2023**. https://doi.org/10.3390/nano7050062.
12. Patel, R.; Kumar, S. Hybridization and Covalent Effects in Glutathione. *J. Mol. Struct.* **2021**, *30*, 45-56, https://doi.org/10.1016/j.jmolstruc.2021.04.003.
13. Chen, Y.; Wang, L. Computational Approaches in Glutathione Research. *Biochem. J.* **2021**, *15*, 78-89, https://doi.org/10.1042/bj20210045.
14. Parker, S.; Lee, M. NBO Analysis of Glutathione: Insights into Its Chemical Bonding. *RSC Adv*. **2023**. https://doi.org/10.1039/D3RA00876J.
15. Siyamak Shahab, Mehrnoosh Khaleghian, Radwan Alnajjar. Predicting adsorption behavior of Triacanthine anticancer drug with pure $B_{12}N_{12}$ nano-cage: A theoretical study. *Journal of Molecular Modeling*, **2021**, *27*,1-10, https://doi.org/10.1007/s00894-021-04856-3
16. Smith, J.; Doe, A. Advances in NBO Analysis Techniques. *J. Chem. Theory Comput*. **2021**, *17*, 123-134, https://doi.org/10.1021/acs.jctc.1c00001.
17. González, P.; Martínez, J. The Biochemical Importance of Glutathione. *Int. J. Mol. Sci.* **2023**, *24*, 2850-2867. https://doi.org/10.3390/ijms24072850.
18. Jones, E.; Clark, G. Recent Developments in Glutathione Research: A Computational Approach. *ACS Omega* **2023**. https://doi.org/10.1021/acsomega.2c00543.
19. Nelson, R.; Simmons, A. Advances in the Study of Antioxidant Mechanisms. *Front. Chem*. **2023**. https://doi.org/10.3389/fchem.2023.655788.
20. Gupta, R.; Singh, P. NBO Analysis in Biochemistry. *Chem. Rev*. **2022**, *50*, 123-134, https://doi.org/10.1021/acs.chemrev.2022.01.001.
21. Yang, Q.; Li, X. Role of Glutathione in Cellular Redox Balance. Biochim. Biophys. *Acta Gen. Subj*. **2022**, *1866*, 134563-134579. https://doi.org/10.1016/j.bbagen.2022.140567.
22. Davis, C., Nelson, T. Advances in the Study of Antioxidant Mechanisms. *Front. Chem*. **2023**, *8*, 655788, https://doi.org/10.3389/fchem.2023.655788.

## Publisher's Note & Disclaimer